JOURNAL OF MATERIALS SCIENCE 30 (1995) 1487–1494

Ignition phenomena and reaction mechanisms of the self-propagating high-temperature synthesis reaction in the Ti+C system

WEI-CHANG LEE, SHYAN-LUNG CHUNG*
Department of Chemical Engineering, National Cheng Kung University, Tainan, Taiwan 70101

The ignition phenomena and the reaction mechanism of the self-propagating high-temperature synthesis reaction of titanium and carbon powders were experimentally investigated. When using coarse graphite powders (< 325 mesh) as the carbon source, the ignition temperature ranged from 1650–1720 °C and was independent of the C/Ti ratio. The ignition temperature could be significantly lowered by using finer graphite powders (e.g. 1400 °C for < 1 μm powder). When using carbon black as the carbon source, the ignition temperature ranged from 1050–1475 °C and was dependent on the C/Ti ratio. The ignition was confirmed in this study to be controlled by the rate of the surface reaction between titanium and carbon which, in turn, was determined by the contact surface area between them. The fractured surfaces of the products showed two different types of morphology, i.e. groups of grains similar to sintered bodies and agglomerated fine particles. The relative quantities of the two types of morphology depended on the type of carbon used, the C/Ti ratio, the particle size of graphite and the density of the reactant pellet. Possible reaction mechanisms have been proposed on the basis of the experimental observations of the ignition phenomena and the product morphology.

1. Introduction

The practical application of a combustion reaction towards synthesizing a refractory material was first considered by Walton and Poulos [1] who produced cermet materials using thermite reactions. Little further development took place until the late 1960s when Merzhanov and co-workers [2–5] initiated research efforts on self-propagating combustion reactions. These research efforts by Merzhanov led to the development of a process, for producing a variety of refractory materials, which they called "self-propagating high-temperature synthesis (SHS)" or, more simply, combustion synthesis. In this process, materials which have sufficiently high heat of formation could potentially be synthesized in a combustion wave, which after ignition, spontaneously propagates throughout the reactants converting them into the products. A wide variety of materials have been produced by this method, including carbides [5, 6], borides [3–7], nitrides [8–10], intermetallics [11, 12], and composite materials [13].

Current interest in such reactions partially stems from claims that materials prepared through this method (combustion synthesis) are superior to those prepared by conventional means [6, 14]. Combustion-synthesized materials are reported to have a higher purity, be more reactive, and possess improved mechanical properties. Higher purity is attributed to the expulsion of impurities as volatile species at the high temperature that is typically attained during these reactions. Meanwhile, the improvements in reactivity and mechanical properties are attributed to the high defect concentrations resulting from both the attainment of high temperature and also the relatively rapid cooling rates following the formation of the products.

Considerable effort has been exerted towards studying, both theoretically and experimentally, the combustion synthesis reactions [15–18]. However, consistent agreement between experimental observations and theoretical predictions is currently insufficient. This insufficiency is primarily the consequence of the numerous simplifying assumptions incorporated into the theoretical models and also a lack of sufficiently detailed experimental investigations.

In this work, the combustion of titanium and carbon powders applied towards producing TiC was selected as a model system for study of the SHS reaction. The effects of various experimental parameters on the ignition temperature and the product morphology were investigated. The heterogeneous nature of the reaction was considered in theoretical analysis and possible reaction mechanisms were proposed.

2. Experimental procedure

The characteristics of the reagents used in the present study are listed in Table I. Titanium powder with

*Author to whom all correspondence should be addressed.

0022–2461

TABLE I The characteristics of the reagents

Reagent	Particle size	Purity (%)	Source
Titanium	− 325 mesh	99.50	Cerac, Inc., USA
Graphite (I)	− 325 mesh	99.90	Carbon Particle Co., Japan
Graphite (II)	< 1 μm	99.99	Johnson Matthey Catalog Co., USA
Carbon Black	~ 0.01 μm	98.00	China Synthetic Rubber Co., Taiwan
TiC	− 325 mesh	99.00	Strem Chemical, Inc., USA

> 95% under 325 mesh was used as the titanium source. Graphite or carbon black powder was used as the carbon source. Two types of graphite powder were used, i.e. one with > 95% under 325 mesh and the other smaller than 1 μm. The carbon black is composed of agglomerates of the sizes ranging from 0.2–1.0 μm and the primary particles of ~ 0.01 μm.

The titanium and carbon powders at the desired atom ratios were thoroughly mixed in ethanol by mechanical stirring at 10^4 r.p.m. for 30 min. After drying by evacuation, the powders were pressed into cylindrical pellets, 10 mm diameter and 5 mm long, by using a steel die with two plungers. The pellets were pressed uniaxially at pressures ranging from 86–100 MPa to obtain densities of 60% ± 5% theoretical. In some of the experiments, TiC powder was added and mixed with the titanium and carbon powders for studying dilution effect.

A schematic diagram of the reaction chamber for the present study is shown in Fig. 1. The reactant pellet was placed on a height-adjustable stage in the reaction chamber. The stage was adjusted so that the top surface of the pellet was approximately 2–3 mm below the tungsten heating coil. The chamber was evacuated to 10^{-1} torr (1 torr = 133.322 Pa) by flushing with argon between the evacuations. After the evacuation, the chamber was filled with argon at 1 atm. The combustion reaction was ignited by heating the top surface of the pellet for several seconds by passing an electric current (500–1000 VA) through the heating coil. The progress of the combustion wave was recorded with a video camera and the temperatures were measured by using 0.127 mm diameter W–W26 % Re thermocouples.

Fig. 2 shows the configuration and location of the thermocouples for ignition temperature measurement. The thermocouple was placed in a narrow groove (0.5 mm wide and 0.2 mm deep) cut into the top surface of the pellet. The signals from the thermocouple were stored and processed by a data acquisition system.

The formation of the product, TiC_x, was determined by X-ray diffraction (XRD) analysis. The morphology of the fractured surface of the pellet (before and after combustion) was analysed by observation with a scanning electron microscope (SEM).

3. Results

Typical temperature–time histories during heating and ignition with three different heating rates are shown in Fig. 3. The temperature at the point of abrupt increase is defined as the ignition temperature.

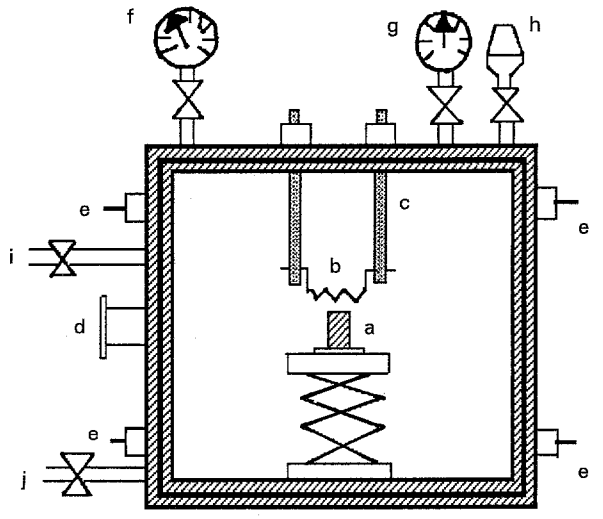

Figure 1 Schematic diagram of the SHS reaction chamber: a, reactant pellet; b, tungsten heating coil; c, graphite rods; d, observation window; e, thermocouple leads; f, pressure gauge; g, vacuum gauge; h, vacuum gauge tube; i, gas outlet; j, gas inlet.

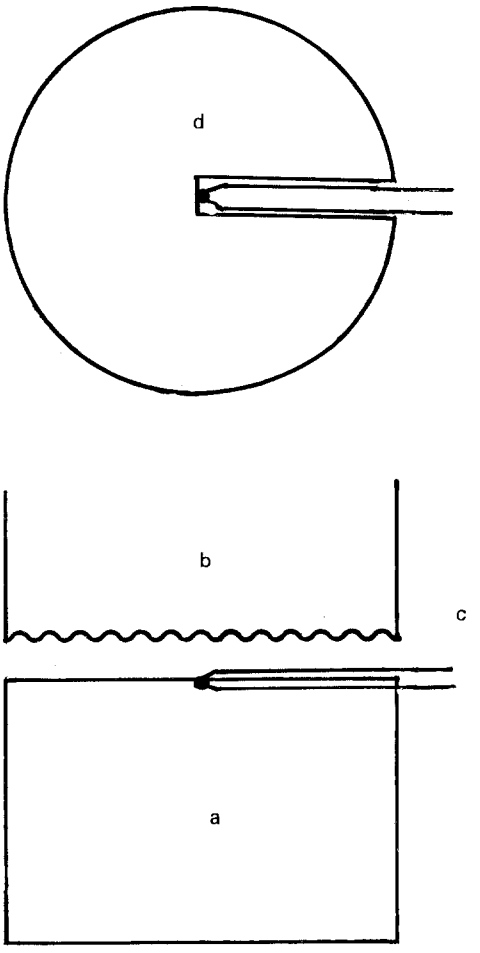

Figure 2 Configuration and location of the thermocouple for ignition temperature measurement: a, reactant pellet; b, tungsten heating coil; c, thermocouple; d, groove.

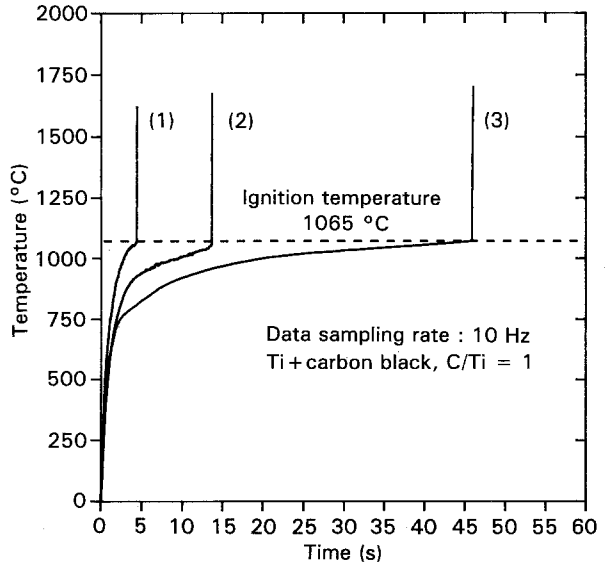

Figure 3 Typical temperature–time histories during heating and ignition. Voltage supplied for heating: (1) 60 V, (2) 55 V, (3) 40 V.

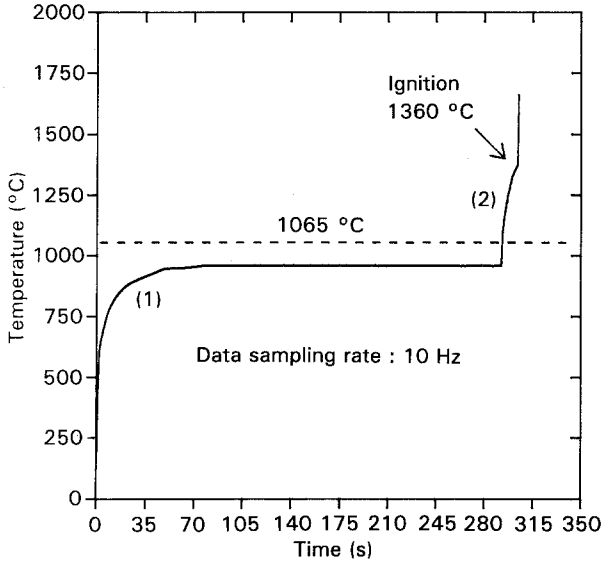

Figure 4 Effect of low heating rate on ignition temperature. Voltage supplied for heating: (1) 35 V, (2) 55 V.

The ignition temperature is found in this figure to remain unaffected by variation of the heating rate (i.e. the voltage supplied for heating varies from 40–60 V and the time of heating for ignition consequently varies from 45–3 s). The ignition temperature can, however, be significantly increased whenever the heating rate is very low. As shown in Fig. 4, when applying a voltage of 35 V, the temperature increased slowly and then remained unchanged at 960 °C. As the voltage was increased to 55 V, the temperature increased quickly and ignition occurred at 1360 °C. Comparing with the cases shown in Fig. 3, the ignition temperature is noted to be increased by 295 °C due to the low heating rate. In two other experiments, similar reactant pellets were used and they were removed from the reaction chamber after heating with a voltage of 35 V for 200 and 1000 s, respectively. The top surfaces of the pellets were analysed for their chemical composition. As indicated by their XRD patterns shown in Fig. 5, formation of TiC began to be detected for the pellet after heating for 200 s. In all the experiments presented hereafter, a voltage of 60 V (when using carbon black) or 70 V (when using graphite) was applied for heating, and ignition occurred in 2–5 s (carbon black) or 20–30 s (graphite). The effect of slow heating on the ignition temperature was thus eliminated.

The ignition temperatures of the Ti + C system are listed in Table II under various experimental conditions. When using carbon black as the carbon source, the ignition temperature ranged from 1050–1475 °C depending on the C/Ti ratio. The ignition temperature was the lowest at C/Ti = 1 and increased at higher or lower ratios. When TiC was added to the reactant pellet, the ignition temperature was increased with a larger extent of increase occurring at higher percentages of addition. When using coarse graphite particles (< 325 mesh), the ignition temperature ranged from 1650–1720 °C. Additionally, the ignition temperature was found to be 1660 °C when 15 wt % TiC was added. Because the uncertainty of the temperature measurement was approximately ± 80 °C, the ignition temperature consequently remained essentially unaffected by the C/Ti ratio and the addition of TiC. However, the ignition temperature was significantly lowered by using finer graphite particles, e.g. 1400 °C for < 1 μm particles.

Fig. 6 shows two scanning electron micrographs of the top surfaces of the reactant pellets of Ti + graphite and Ti + carbon black, respectively. As can be seen, the contact surface area between titanium and carbon black is much larger than that of titanium and graphite. The fractured surfaces of the products show two different types of morphology, i.e. groups of grains similar to sintered bodies, and agglomerated fine particles (Fig. 7). Relative quantities of the two types of morphology depend upon the type of carbon used, the C/Ti ratio, the particle size of graphite and the density of the reactant pellet. Lower C/Ti ratio or/and the use

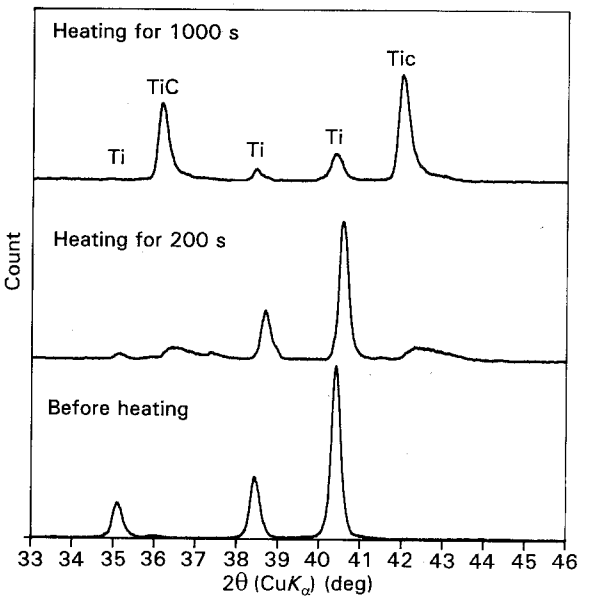

Figure 5 XRD patterns of the top surfaces of the reactant pellets before and after heating. Ti + carbon black, and C/Ti = 1.

TABLE II Ignition temperatures under various operating conditions

Ti(< 325 mesh) + CB[a]	Ignition temp. (°C)	Ti(< 325 mesh) + Gr[b] (< 325 mesh)	Ignition temp. (°C)	Ti(< 325 mesh) + CB, C/Ti = 1	Ignition temp. (°C)
C/Ti = 0.5	1475	C/Ti = 0.8	1720	0% TiC added	1050
C/Ti = 0.75	1350	C/Ti = 1.0	1700	20% TiC added	1390
C/Ti = 0.85	1193	C/Ti = 1.3	1650	30% TiC added	1427
C/Ti = 1.0	1050	C/Ti = 1, 15% TiC added	1660	40% TiC added	1470
C/Ti = 1.5	1380	Ti(< 325 mesh) + Gr(< 1 μm)	1400		
C/Ti = 2.0	1415	C/Ti = 1.0			

[a] CB, carbon black.
[b] Gr, graphite powder.

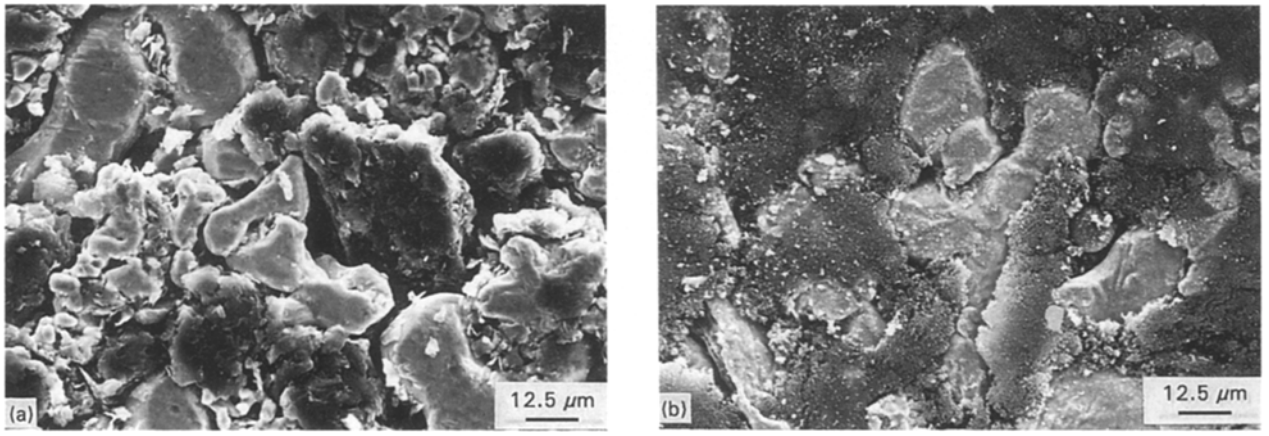

Figure 6 Scanning electron micrographs of the top surfaces of the reactant pellets: (a) Ti + graphite; (b) Ti + carbon black.

of graphite particles favours the formation of sintered-grain structure (compare Fig. 7a–d). When using graphite as the carbon source, lower pellet density (i.e. 30% theoretical) or/and the use of finer particles (< 1 μm) favours the formation of agglomerated fine particles (Fig. 7e and f). Fig. 8a is a scanning electron micrograph of a fractured surface of a pellet with low degree of conversion due to the addition of 15 wt % TiC as diluent. The sintered-grain structure forming the circle was identified as TiC while those inside the circle were identified as unreacted graphite particles which had been spread over by titanium, thus appearing smooth in boundaries. Fig. 8b is a scanning electron micrograph of a fractured surface of another pellet with a high degree of conversion, showing a similar structure. The sintered grain structure forming the circle was also identified as TiC. However, those inside the circle were agglomerated fine particles which were identified as TiC. The degree of conversion of the Ti + C system under various experimental conditions has been studied previously [19]. It was found that the degree of conversion remained essentially constant at approximately 99.8% with C/Ti ranging from 0.85–1.1 and that it decreased to 96.5% at C/Ti = 0.65.

4. Discussion

4.1. Theoretical analysis

The temperature variation of the top surface of a reactant pellet during heating and ignition can be described by the following energy equation

$$\rho C_p \, dv \frac{dT}{dt} = \dot{Q}_{ext} + \dot{Q}_{r \times n} \, dv - \dot{Q}_{loss} \qquad (1)$$

where ρ is the density of the pellet, dv is the control volume at the top surface of the pellet where ignition occurs, C_p is the heat capacity, T is the temperature at time t, $\dot{Q}_{ext}$ is the rate of heat transferred to the control volume by external heating, $\dot{Q}_{loss}$ is the rate of heat loss, and $\dot{Q}_{r \times n}$ is the rate of heat generation by reaction per unit volume within the control volume. Before the onset of combustion, because the reaction takes place predominately at the contact surface between the reactant particles, $\dot{Q}_{r \times n}$ can be expressed as

$$\dot{Q}_{r \times n} = HS\alpha \exp\left(-\frac{E}{RT}\right) \qquad (2)$$

where H is the heat of reaction per mole of product formed, S is the contact surface area per unit volume of the pellet, α is the pre-exponential factor, and E is the activation energy of the reaction.

Ignition occurs when the reaction rate is high enough so that the rate of heat generation ($\dot{Q}_{r \times n} \, dv$) is larger than the rate of heat loss ($\dot{Q}_{loss}$). Under such circumstances, the temperature of the control volume increases continuously even with the removal of the external heating. The increase in temperature substantially increases the reaction rate which, in turn, causes

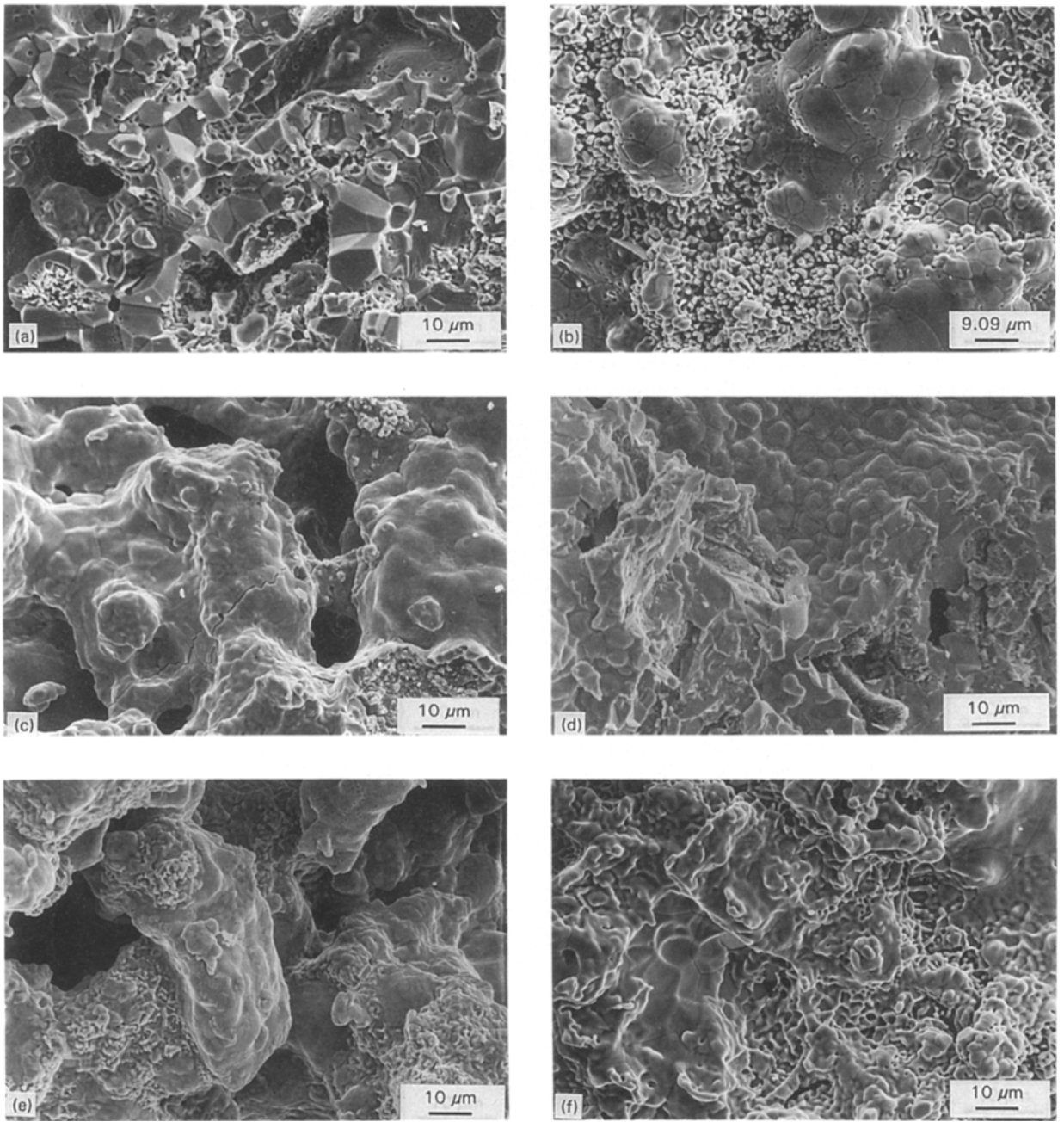

Figure 7 Scanning electron micrographs of the fractured surfaces of the products. (a) Ti + graphite (< 325 mesh), C/Ti = 1; (b) Ti + carbon black, C/Ti = 1; (c) Ti + graphite (< 325 mesh), C/Ti = 0.7; (d) Ti + carbon black, C/Ti = 0.6; (e) Ti + graphite (< 1 μm), C/Ti = 1; (f) Ti + graphite (< 325 mesh), C/Ti = 1, low pellet density (30% theoretical).

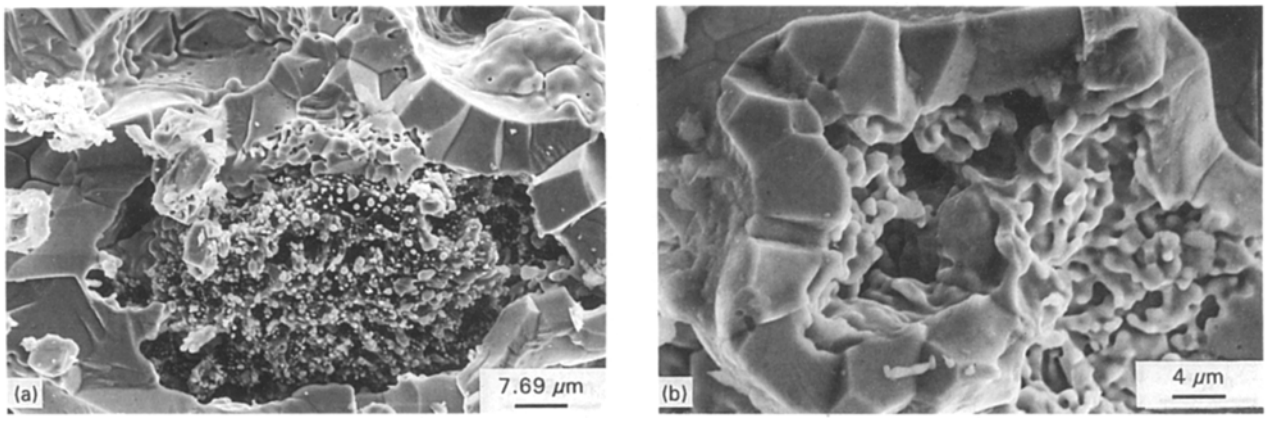

Figure 8 Scanning electron micrographs of the fractured surfaces of the products: (a) Ti + graphite (< 325 mesh) + 15 wt % TiC, C/Ti = 1; (b) Ti + graphite (< 325 mesh), C/Ti = 1.

the temperature to increase further. This occurs because the reaction rate is a strong function of temperature. This mutual effect rapidly brings the reaction to proceed vigorously, thus the onset of combustion or ignition takes place.

4.2. Effect of contact surface area

For a particular system, e.g. the reaction between titanium and carbon particles in the present study, the values of H, α and E in Equation 2 can be taken as constant. The reaction rate is thus determined by the combination effect of two variables, i.e. temperature and the contact surface area between the reactant particles. A lower temperature, i.e. the ignition temperature, is required for a larger contact surface area to enable a particulate reaction rate to be reached for ignition to occur. The contact surface area between titanium and carbon black particles is much larger than that between titanium and graphite particles. Consequently, the ignition temperature of titanium and carbon black is much lower than that of titanium and graphite. When adding TiC to the mixture of titanium and carbon black and/or selecting the C/Ti ratios other than 1, the contact surface area is decreased which consequently results in a higher ignition temperature. The SHS reaction of the Ti + C system is indicated from several other investigations [13, 18, 20] to correlate markedly with the melting of titanium particles which results in the capillary spreading. The ignition temperature was found in the present study to be dependent upon the size of the graphite particles. When using coarse particles (< 325 mesh), the ignition temperatures under various C/Ti ratios and with the addition of TiC can all be taken to be the melting point of titanium (1680 °C), because the temperature variations are within experimental error. The contact surface area between titanium and coarse graphite particles is so insignificantly small that the ignition cannot occur until the temperature reaches the melting point of titanium. At its melting point, titanium melts and spreads over the graphite particles. The contact surface area is thus substantially increased, which results in ignition. When adding TiC to the titanium and graphite mixture or selecting C/Ti ratios other than 1, ignition also occurs at the melting point because the titanium melting and spreading to increase the contact surface area is equally required. However, when finer graphite particles (< 1 μm) were used, ignition occurred at 1400 °C due to larger contact surface area.

4.3. Effect of heating rate

The ignition temperature can be significantly increased by applying a low heating rate (see Fig. 4). Because the contact surface area should not be significantly altered by a slow heating, change in the activation energy is thus the primary reason for the increase in the ignition temperature. During slow heating, TiC layers are formed at the interfaces between titanium and carbon particles (Fig. 5), spatially separating the reagents. This imposes a restriction on atom diffusion thus inhibiting further reaction. This effect can be considered as an increase in the activation energy, E. A higher ignition temperature is consequently required in order to reach a particular reaction rate for ignition to occur.

4.4. Reaction mechanism and product morphology

As shown in Figs 9 and 10, possible reaction mechanisms were deduced based on the experimental results. When using carbon black (or fine graphite

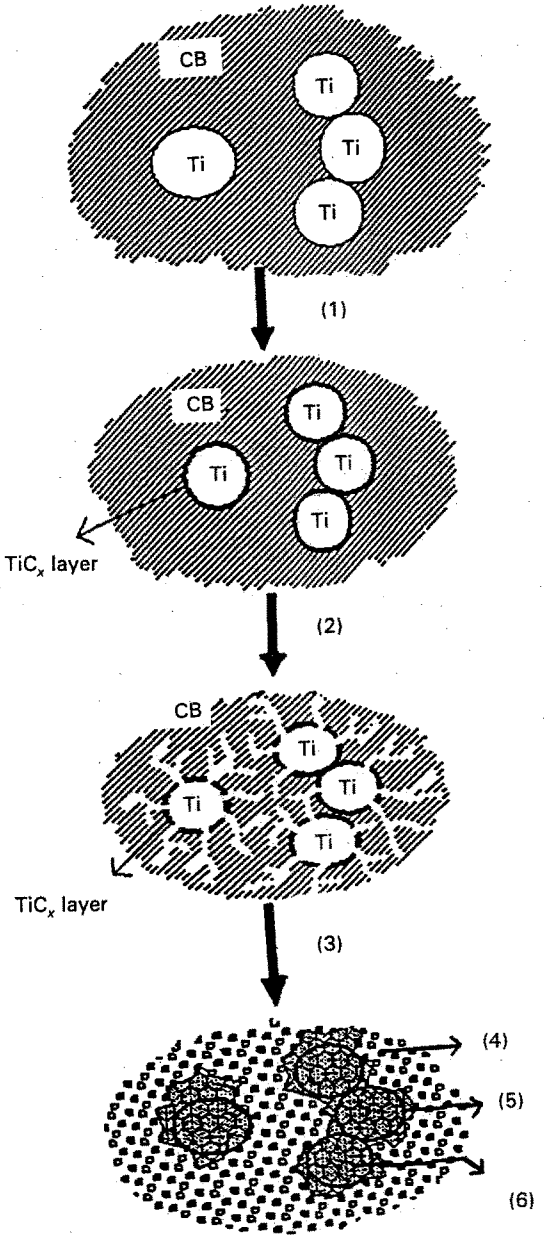

Figure 9 The proposed mechanism of ignition and reaction of titanium and carbon black (CB). (1) Ignition by surface reaction leading to formation of TiC_x layers. (2) Titanium melts as the temperature reaches its melting point; previously formed TiC_x layers dissolve into titanium; liquid titanium infiltrates into the pores of CB; carbon diffuses through the TiC_x layer to react with titanium. (3) Reaction occurs both in the bulk titanium phase and in the CB matrix. (4) Formation of agglomerated fine particles. (5) Original titanium particle boundaries. (6) Formation of sintered-grain structure.

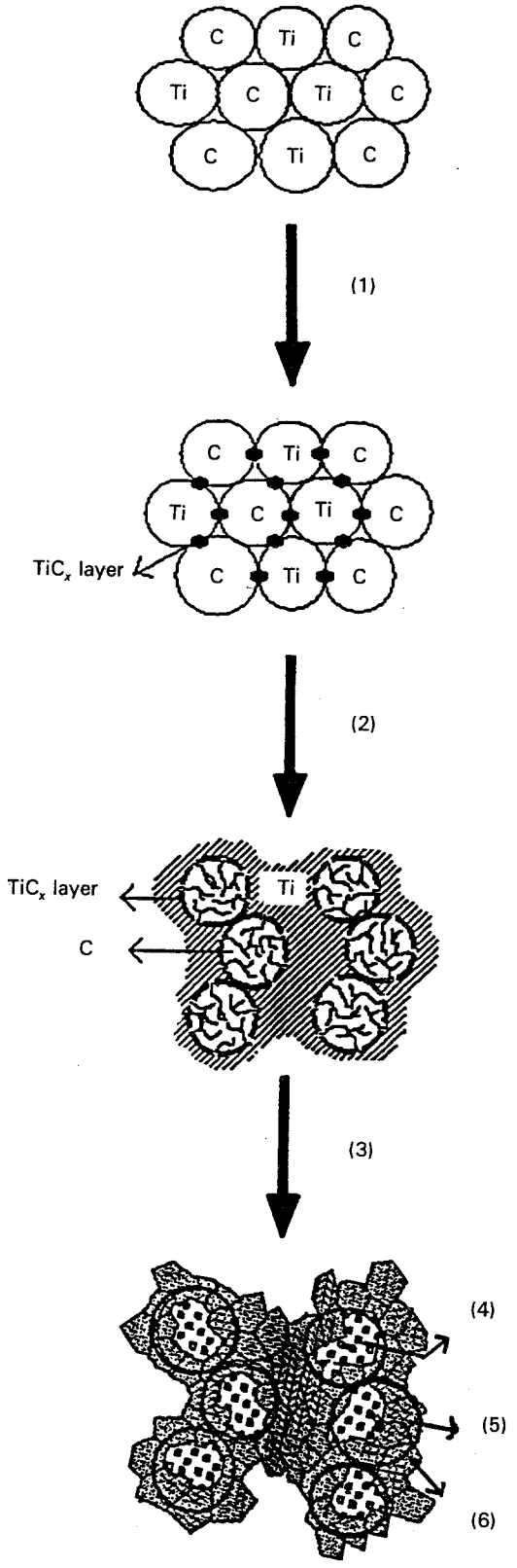

Figure 10 The proposed mechanism of ignition and reaction of titanium and graphite particles. (1) TiC_x layers form at contact spots between titanium and graphite particles. (2) As the temperature reaches the melting point of titanium, titanium melts, spreads over graphite particles and fills in the pores; ignition occurs resulting in the formation of TiC_x layers; carbon diffuses through the TiC_x layer to react with titanium and the TiC_x layer dissolves into titanium. (3) Reaction occurs both in the bulk titanium phase and in inter- and intraparticle pores of graphite. (4) Formation of agglomerated fine particles. (5) Original graphite particle boundaries. (6) Formation of sintered grain structure.

particles) as the carbon source, ignition is triggered by surface reaction resulting in the formation of TiC layers at the interfaces between titanium and carbon particles. Further reaction requires transport of reactants through the TiC layer. Previous studies [21–23] showed that the diffusion coefficient of carbon in TiC is approximately three orders of magnitude greater than that of titanium in TiC. Diffusion of carbon through the TiC layer is thus considered as the primary process for the transport of the reactants. After ignition, the temperature increases rapidly to the melting point of titanium. Consequently, the TiC layer does not grow to a thickness significantly retarding the reaction, because at its melting point, titanium melts and the TiC layers dissolve into it. Subsequently, titanium melt infiltrates the pores of the carbon black and spreads over the carbon particles. Pampuch *et al.* [24] studied the combustion reaction of the Si–C system and concluded that in order to ensure a high rate of reaction as a combustion mode, a thin SiC layer would have to be retained. This required the rate of dissolution of SiC in the silicon melt to be no smaller than the rate of the formation of the SiC layer. They also proposed that the product SiC was formed by crystallization from the silicon melt due to supersaturation. A similar reaction mechanism is considered in the present study. Fig. 11 is a schematic diagram of the structure of the interface between the reactants. The composition variation across the TiC_x layer is indicated by the attached phase diagram [25] of the Ti–C system. The concentration gradient of

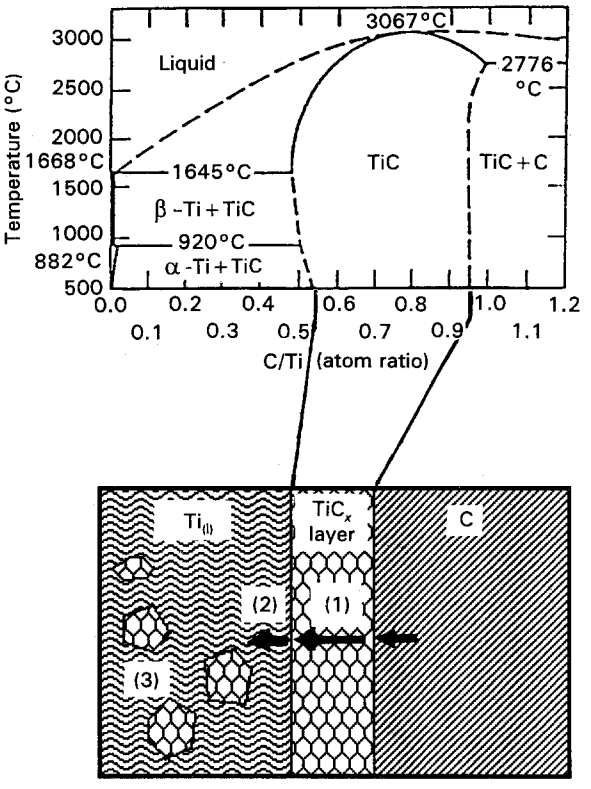

Figure 11 A schematic diagram of the structure of the interface between titanium and carbon. (1) Diffusion of carbon through the TiC_x layer, (2) dissolution of TiC_x into the titanium melt, (3) TiC formed by crystallization.

carbon across the TiC_x layer provides a driving force for the diffusion of carbon through it. Although TiC is continuously formed at the Ti–TiC_x interface, a thin TiC_x layer is retained due to its simultaneous dissolution in the titanium melt. The reaction forming TiC takes place both in the bulk titanium phase (the original titanium particles) and in the carbon black matrix. In the bulk titanium phase, TiC is formed by crystallization due to supersaturation, and subsequent growth of the nuclei leads to the formation of the sintered grain structure. In the carbon black matrix, TiC is also formed by crystallization. However, because growth of the nuclei in the pores is limited, it appears as agglomerated fine particles.

In the case of using coarse graphite particles, ignition occurs at the melting point of titanium, at which titanium melt spreads over the graphite particles and infiltrates into their micropores (i.e. intraparticle pores). The structure of the interface between the reactants, the diffusion and reaction processes are all similar to the case of using carbon black as described previously. The TiC formed in the bulk titanium phase has the sintered grain structure, while those formed in the inter- and intraparticle pores of graphite are agglomerated fine particles (compare Fig. 8a and b).

Because the carbon black contains many more pores than does the graphite, the TiC produced with carbon black contains more agglomerated fine particles (compare Fig. 7a and b). When using lower C/Ti ratios, because fewer pores are available, it favours the formation of sintered grain structure (compare Fig. 7a–d). Under the conditions of lower pellet density and/or using finer graphite particles, more agglomerated fine particles are formed because more pores are available (compare Fig. 7a, e and f). The effects of the experimental parameters on the product morphology can thus be explained by the proposed mechanisms.

5. Conclusion

Possible ignition and reaction mechanisms of the SHS reaction between titanium and carbon powders have been proposed. Occurrence of the ignition is controlled by the rate of the surface reaction between titanium and carbon particles which, in turn, is determined by the contact surface area between them. Reactants with larger contact surface areas require lower ignition temperatures. However, preheating or applying a lower heating rate results in an increase in ignition temperature due to the increase in activation energy. The proposed mechanisms can explain the formation of the two types of morphology of the product. The reaction occurring in the bulk titanium phase produces the sintered grain structure, and that occurring in the inter- and intraparticle pores of carbon produces the agglomerated fine particles.

Acknowledgement

Support of this research by the National Science Council, Taiwan under grant NSC-82-0402-E006-232 is gratefully acknowledged.

References

1. J. D. WALTON and N. E. POULOS, *J. Am. Ceram. Soc.* **42** (1959) 40.
2. A. G. MERZHANOV and I. P. BOROVINSKAYA, *Dokl. Akad. Nauk. SSSR (Chem.)* **204** (1972) 366.
3. I. P. BOROVINSKAYA, A. G. MERZHANOV, N. P. NOVIKOV and A. K. FILONENKO, *Combust. Explos. Shock Waves* **10** (1974) 2.
4. A. G. MERZHANOV, A. K. FILONENKO and I. P. BOROVINSKAYA, *Dokl. Akad. Nauk. SSSR (Chem.)* **208** (1973) 892.
5. A. G. MERZHANOV, G. G. KARYUK, I. P. BOROVINSKAYA, V. K. PROKUDINA and E. G. DYAD'KO, *Sov. Powder Metall. Met. Ceram.* **20** (1981) 709.
6. J. B. HOLT and Z. A. MUNIR, *J. Mater. Sci.* **21** (1986) 251.
7. A. A. ZENIN, A. G. MERZHANOV and G. A. NERSISYAN, *Fiz. Goren. Vzryva* **17** (1981) 63.
8. Z. A. MUNIR and J. B. HOLT, *J. Mater. Sci.* **22** (1987) 710.
9. I. P. BOROVINSKAYA and V. E. LORYAN, *Sov. Powder Metall. Met. Ceram.* **191** (1979) 851.
10. T. M. MAKSIMOV, M. K. ZIATDINOV, A. G. RASKOLENLO and O. K. LEPAKOVA, *Combust. Explos. Shock Waves* **15** (1979) 415.
11. A. R. SARKISYAN, S. K. DOLUKHANYAN and I. P. BOROVINSKAYA, *Sov. Powder Metall. Met. Ceram.* **17** (1978) 424.
12. K. A. PHILPOT, Z. A. MUNIR and J. B. HOLT, *J. Mater. Sci.* **22** (1987) 159.
13. S. D. DUNMEAD, D. W. READEY, C. E. SEMLER and J. B. HOLT, *J. Am. Ceram. Soc.* **72** (1989) 2318.
14. O. R. BERGMANN and J. BARRINGTON, *ibid.* **49** (1966) 502.
15. A. P. HARDT and P. V. PHUND, *Combust. Flame* **21** (1973) 77.
16. A. P. HARDT and R. W. HOLSINGER, *ibid.* **21** (1973) 91.
17. V. O. ERAMKOV, A. G. STRUNINA and V. V. BARZYKIN, *Combust. Explos. Shock Wave* **12** (1976) 185.
18. S. C. DEEVI, *J. Mater. Sci.* **26** (1991) 2662.
19. W. C. LEE and S. L. CHUNG, *Int. J. Self-Propagat. High-Temp. Synth.* **1**(2) (1992) 211.
20. A. I. KIRDYASHKIN, YU. M. MAKSIMOV and E. A. NEKRASOV, *Fiz. Goren. Vzryva* **17**(4) (1981) 33.
21. S. SARIAN, *J. Appl. Phys.* **39** (1968) 3305.
22. *Idem, ibid.* **39** (1968) 5036.
23. *Idem, ibid.* **40** (1969) 3515.
24. R. PAMPUCH, J. LIS and L. STOBIERSKI, in "Combustion and Plasma Synthesis of High Temperature Materials", edited by Z. A. Munir and J. B. Holt (VCH, New York, 1990) p. 211.
25. E. K. STORMS, in "The Refractory Carbides", edited by J. L. Margrave (Academic Press, New York, 1967) p. 3.

Received 8 November 1993
and accepted 9 June 1994